Experimental Astronomy (2024) 57:12
https://doi.org/10.1007/s10686-024-09931-1

RESEARCH

How many random observations are needed for good phase coverage of a periodic source?

Chris Koen[1]

Received: 25 September 2023 / Accepted: 22 February 2024 / Published online: 9 March 2024

Abstract

The specific problem considered is the number of radial velocity measurements required to obtain good estimates of physical parameters of binary star. It is assumed that observations are made at random binary phases. The loss of information due to poor phase coverage is explored, and a suggested limit on the largest acceptable gap introduced. The statistical distribution of maximum gap lengths can then be used to specify the minimum number of velocity measurements to obtain good phase coverage with a specified confidence limit. The effects of non-zero orbital eccentricity are discussed, as are the ramifications of having multiple binary targets. The theory is also applicable to the characterisation of the radial velocity curves induced by exoplanets on their host stars, provided that the periods and eccentricities are known (from e.g. transit observations).

Keywords Radial velocity measurements · binary stars · astrostatistics · stars: planetary systems

1 Problem statement

Consider the following project: radial velocities of a number of faint binary star targets are to be obtained by queue scheduling of observing time. The scheduling will be such that measurements will be obtained at random phases. (For example, the periods may be much shorter than times between observations). How many visits N per target are required to ensure good phase coverage? It is assumed that the period P and the orbital eccentricity e of each of the stars is known from photometric measurements.

✉ Chris Koen
ckoen@uwc.ac.za

[1] Department of Statistics, University of the Western Cape, Private Bag X17, Bellville, 7535 Cape, South Africa

In general, the radial velocity is described by the set of equations

$$\begin{aligned}
M &= \frac{2\pi}{P}(t - t_0) \\
M &= E - e\sin\ E \\
\theta &= 2\tan^{-1}\left[\sqrt{\frac{1+e}{1-e}}\tan(E/2)\right] \\
v_r &= \gamma + K[\cos(\theta + \omega) + e\cos\omega]
\end{aligned} \tag{1}$$

where γ is the systemic velocity, K the semi-amplitude, $\theta = \theta(t)$ the true anomaly, ω the argument of periastron, E the eccentric anomaly, M the mean anomaly, and t_0 the time of periastron passage [e.g. Tatum [13] or https://www.astro.uvic.ca/~tatum/celmechs.html]. This serves as a basis for the material below.

It is well known that the eccentricity of binary orbits can be determined from light curves alone (e.g. [12]). Approximate eccentricities of exoplanetary orbits can also be calculated from photometry of transits. If more than one planet orbits a star, the transit timings will not be perfectly periodic. The transit timing variations can be used to infer, amongst other quantities, the eccentricities of the planetary orbits (e.g. [1, 4, 6]). The effects of eccentricity on the shape of transit light curves have also been exploited to derive a relationship between the eccentricity and the mean density of the host star (e.g. [2, 7], and references therein). Weak limits on the stellar density lead to sharp limits on the eccentricity of the planetary orbit.

The conclusion is that information (periods, eccentricities) gained from transit observations can be also used to plan radial velocity observations of exoplanet systems. Given that the velocities involved are much smaller than those of binary stars, the theory below pertains to the minimum number of *epochs* of observation, rather than the total number of velocity measurements.

2 Adequate phase coverage

The first task is to define what exactly is meant by “good" (or adequate) phase coverage. A sensible approach is to base the answer on controlling the estimation errors on the parameters of interest (systemic, velocity, velocity semi-amplitude and argument of periastron, if $e = 0$.)

A quantitative answer to the question can be given by noting that for circular orbits, the observed radial velocity is

$$v_r(t) = \gamma + K\cos(2\pi t/P + \omega') + \varepsilon(t)$$

where ω' is the phase at time $t = 0$ and ε represents measurement error. If the velocities are phased with respect to P,

$$\begin{aligned}
v_r(t) &= \gamma + K\cos[2\pi\psi(t) + \phi] + \varepsilon(t) \\
&= \gamma + A\cos[2\pi\psi(t)] + B\sin[2\pi\psi(t)] + \varepsilon(t)
\end{aligned} \tag{2}$$

with $0 \leq \psi < 1$. Equation (2) is in standard linear regression form; it follows immediately that the covariance matrix C of the estimated values of γ, A and B is

$$C = \sigma_\varepsilon^2 (X'X)^{-1} \equiv \sigma_\varepsilon^2 W \tag{3}$$

(e.g. [8]). In this case the design matrix X is

$$X = \begin{bmatrix} 1 & \cos 2\pi\psi_1 & \sin 2\pi\psi_1 \\ 1 & \cos 2\pi\psi_2 & \sin 2\pi\psi_2 \\ \vdots & \vdots & \\ 1 & \cos 2\pi\psi_N & \sin 2\pi\psi_N \end{bmatrix}. \tag{4}$$

The considerable advantage of the linear form in (2) is that X, and hence W, does not contain any unknowns: scale factor σ_ε aside, C is fully characterised by W.

The statistical field of optimal design is concerned with controlling (as much as possible) the entries in X in order to minimise the variances appearing in the matrix C. To this end, various measures based on the matrix W has been suggested. Here, we will refer to only two popular choices: A-optimality, which entails minimising the trace of W, and D-optimality, which minimises the determinant of W (e.g. [10]).

Figures 1 and 2 illustrate application of the two optimality criteria to the problem at hand. Proceeding from a regular grid of phase values ψ spanning the interval [0, 1), gaps are introduced, as plotted in Fig. 1. Gaps are increased in length, and for each "design" the matrix W is calculated. The traces and determinants of W are plotted in Fig. 2, normalised with respect to the values for zero gap length. As expected, trace(W)

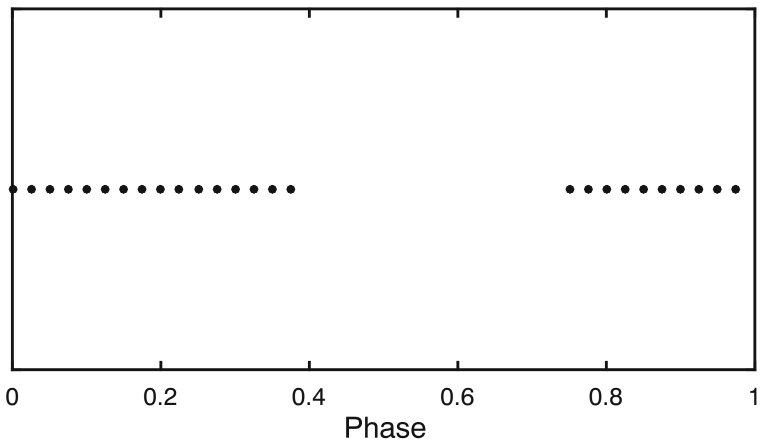

Fig. 1 The pattern of phase spacings used to derive the results in Fig. 2: a regular grid spacing covering the interval [0, 1), with a single large gap

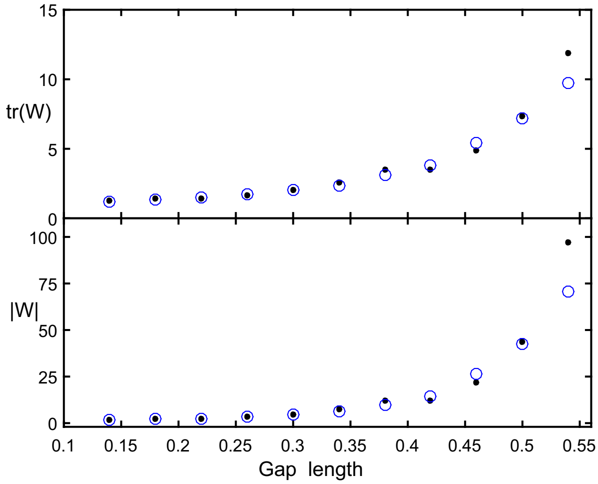

Fig. 2 The effect of large gaps in a regularly spaced coverage of the phase interval [0, 1), as in Fig. 1. Top panel: the A-optimal criterion. Bottom panel: D-optimal criterion. Dots and circles respectively show results for full observation grids of 20 and 60 points

and $|W|$ increase with increasing gap lengths, demonstrating the sub-optimality with respect to the complete set of phases ψ.

The interpretation of the A-optimality criterion is more transparent: it is essentially the sum of the three variances (of the estimated values of γ, A and B). For gap lengths longer than 0.45, trace$(W) > 5$, i.e. a five-fold increase in the variance. The precise choice will obviously be dependent on the context. Here, illustrative numerical values will be given assuming maximum acceptable phase gaps of 0.4.

3 Probability of large gaps

It is convenient to think of phase as being defined on a circle with unit circumference, so that ψ and $\psi + k$, with k being any integer, refer to the same radial velocity phases. The phase of each radial velocity measurement corresponds uniquely to a point placed randomly on the unit circle. The definition of good phase coverage is then equivalent to placing a limit ℓ on the largest arc length between any two points on the unit circle. This problem appears to have been first addressed by Stevens [11]. We will use the result (e.g. [5])

$$F(\ell) = \sum_{j=0}^{L} (-1)^j \binom{N}{j} (1 - j\ell)^{N-1} \tag{5}$$

where F is the cumulative distribution function (CDF), and $L = \lfloor 1/\ell \rfloor$ is the greatest integer smaller than, or equal to, $1/\ell$.

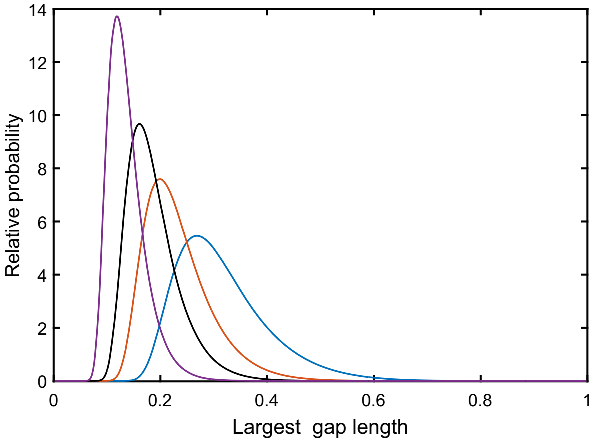

Fig. 3 Probability density functions of ℓ [Equation (6)]. From right to left, $N = 5, 10, 15, 25$

The probability density function (PDF) corresponding to (5) is

$$f(\ell) = N(N-1)\sum_{j=1}^{L}(-1)^{j-1}\binom{N-1}{j-1}(1-j\ell)^{N-2} \,. \tag{6}$$

A few examples are plotted in Fig. 3. As intuition would suggest, PDFs are more compact and concentrated at smaller ℓ as N increases. Note that gaps of length 0.4 are unlikely by the time $N = 15$, and seem virtually impossible at $N = 25$.

Two notes: first, although the shapes of the PDFs in Fig. 3 resemble those of skew normal distributions, the standardised skewness coefficient $\gamma_1 < 1$ for the latter, while the skewness associated with the PDF f slightly exceeds unity for $N \geq 10$. Second, Holst [5], amongst others, discussed the asymptotic distribution of the largest arc length. Although this has a conveniently simple form, numerical experiments show that it is not a good approximation to (5) for the relatively small values of N considered here.

For $0.34 < \ell < 0.5$, $L = 2$ and

$$F(\ell) = 1 - (N-1)(1-\ell)^{N-1} + \frac{1}{2}N(N-1)(1-2\ell)^{N-1} \,.$$

For $\ell = 0.4$, $F(\ell) = 0.989$ for $N = 15$, i.e. in only 1% of cases will phase gaps larger than 0.4 be encountered if v_r is measured 15 times. A 99.9% certainty that $\ell < 0.4$ requires $N = 21$.

4 Several stars

The treatment up to this point has focussed on single targets. Consider a group of M stars, each with N measurements of v_r taken at random phases. Let p be the probability

Table 1 Probabilities of finding 0, 1 or 2 stars with inadequate phase coverage (largest gap ≥ 0.4)

M	$m = 0$		$m = 1$		$m = 2$	
	$N = 15$	$N = 21$	$N = 15$	$N = 21$	$N = 15$	$N = 21$
5	0.946	0.996	0.053	0.004	0.001	0
10	0.896	0.993	0.099	0.007	0.005	0
20	0.802	0.986	0.178	0.014	0.019	1E-4
50	0.576	0.964	0.320	0.035	0.087	6E-4

The number of measurements is N, for each of the M stars

of an unacceptably large phase gap for a single star. Then the probability that m of the M stars will have poorly determined parameters has a binomial distribution:

$$P(m = x) = \binom{M}{x} p^x (1 - p)^{M-x} \tag{7}$$

Table 1 contains some illustrative results: with $N = 21$ random measurements per star there is an reasonable (95%) chance that all M datasets will be acceptable (at least for $M \leq 50$).

5 Non-circular orbits

The problem is somewhat more complicated if the eccentricity $e \neq 0$. Note first though that the last of equations (1) can still be written as a linear regression, albeit in terms of θ, rather than t or ψ:

$$v_r[\theta(t)] = \gamma' + K \cos[\theta(t) + \omega] + \varepsilon(t)$$

with $\gamma' = \gamma + e \cos(\omega)$. This means that the discussion in Section 2 applies, with a limit on the maximum gap in the phased values of true anomaly to be specified. We assume the same numerical value, 0.4, as in Section 2.

The main problem introduced by the non-zero eccentricity is that, contrasting with the case $e = 0$, the random time points of observation do not map into a uniform distribution of phase values. Instead, the distribution is given by the Jacobian of the transformation from ψ to θ (e.g. [9]):

$$\begin{aligned}
f_\theta(\theta) &= \left| \frac{d\psi}{d\theta} \right| \\
&= \left| \frac{d\psi}{dE} \frac{dE}{d\theta} \right| \\
&= \frac{1}{2\pi}(1 - e\cos\ E)\frac{d}{dt}\left\{2\tan^{-1}\left[\alpha\tan(\theta/2)\right]\right\} \\
&= \frac{1}{2\pi}\left\{1 - e\cos\left[2\tan^{-1}(\alpha\tan(\theta/2)\right]\right\}\frac{\alpha}{\cos^2(\theta/2) + \alpha^2\sin^2(\theta/2)}
\end{aligned}$$

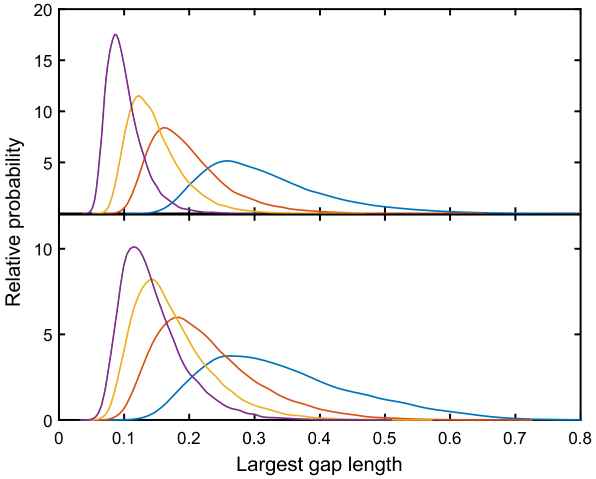

Fig. 4 Simulated probability density functions of ℓ for elliptical orbits. Top panel: $e = 0.2$; from right to left $N = 10, 20, 30, 50$. Bottom panel: $e = 0.5$; from right to left $N = 15, 30, 45, 60$

where $\alpha \equiv \sqrt{(1-e)/1+e)}$ and $-\pi \leq \theta < \pi$. It is slightly more convenient to work in terms of $0 \leq \phi = (\theta + 2\pi)/2\pi < 1$, in which case

$$f_\phi(\phi) = \left\{1 - e\cos\left[2\tan^{-1}(\alpha\cot(\pi\phi)\right]\right\} \frac{\alpha}{\sin^2(\pi\phi) + \alpha^2\cos^2(\pi\phi)} . \qquad (8)$$

A few examples of the largest gap PDFs resulting from (8) are plotted in Fig. 4. In order to produce these, many datasets of size N were simulated from (8), and the largest gap in the ordered phases ϕ for each determined. PDFs were then estimated by a kernel density procedure applied to the collection of largest gaps. Unsurprisingly, considerably larger N, as compared with the $e = 0$ case, are required to thoroughly cover the full phase range (compare Fig. 3). This point is further explored in Table 2 which gives, for a variety of eccentricities, values of N needed to guarantee acceptably small phase gaps.

Table 2 The number of observation N required to ensure a probability p of a maximum gap $\ell = 0.4$ in the true anomaly θ, for different values of the eccentricity e

p	Eccentricity e									
	0	0.1	0.2	0.3	0.4	0.5	0.6	0.7	0.8	0.9
0.05	12	13	14	17	22	28	40	62	114	325
0.01	15	17	20	24	30	40	57	89	165	472
0.001	21	22	27	33	42	57	82	125	233	670

Each entry in the Table is the result of 40000 draws of sample size N from the PDF (8)

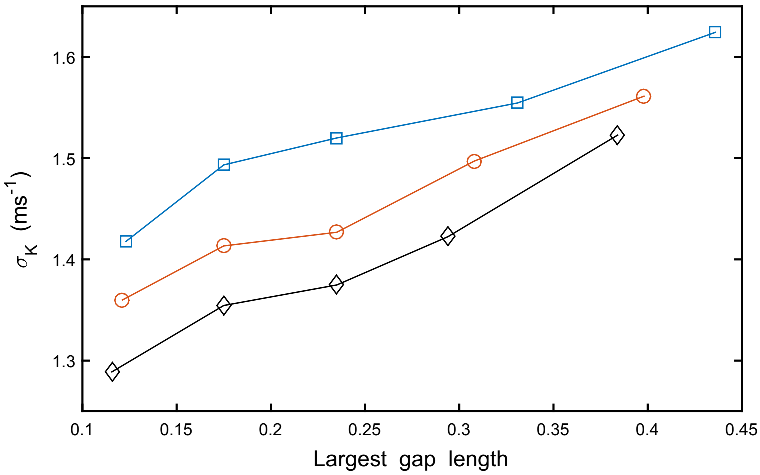

Fig. 5 Standard errors σ_K on the velocity semi-amplitude estimated from subsamples of measurements by Gorrini et al. [3]. Squares, circles and diamonds respectively denote subsamples of size $N = 16$, 18 and 20

6 An illustation

The central point of this paper is illustrated by subsampling radial velocity measurements of the planet-hosting star GJ 3988 [3]. The $P = 6.944$ d orbit of GJ 3988b is circular, so that the discussion in Section 3 applies.

Gorrini et al. [3] obtained 164 velocity measurements, of which three values deviating more than 15 ms^{-1} from the mean were discarded. Small subsamples were randomly drawn from the remaining 161 velocities, such that the times of observation were at least $P/2 = 3.472$ d apart. For each subsample the velocity semi-amplitude K was calculated, and the maximum phase gap ℓ noted. Of interest is the dependence on ℓ of the uncertainty σ_K of the semi-amplitude. This was found be drawing many (10^5) subsamples for a given value of N, binning together those K with similar values of ℓ, and calculating the bin standard deviations. The results can be seen in Fig. 5, which shows the expected monotonic increases of σ_K with ℓ.

7 Concluding remarks

In order to keep the discussion above as simple and general as possible, fitting radial velocity models to observations has been treated as a linear least squares problem. In practice, this would not lead to direct estimation of quantities of interest such as K and ω. In order to estimate these, and other parameters explicitly, nonlinear regression is required, and error estimates would depend on the parameters of each individual system.

In general, Equations (7) and (5) should provide a good guideline for the minimum number of visits to each target. Adhering to those criteria will help guard against estimation errors induced by insufficient phase coverage of binary/exoplanet orbits.

In implementation, Equation (7) can first be used for the specified number of targets M to place a limit on the probability p. The number of visits N can then be solved for from Equation (5). Of course, objects with substantially eccentric orbits will require more visits, and will have to be treated on an individual basis. Furthermore, in the case of exoplanets, random errors (corresponding to the scale factor σ_ε) will play a more important role, necessitating repeated measurements at each target visit.

Acknowledgements Comments from the referee helped the author to improve the paper.

Funding Open access funding provided by University of the Western Cape.

Data Availability The radial velocity data used in Section 6 are from Gorrini et al. [3], and are available from https://cdsarc.cds.unistra.fr/viz-bin/cat/J/A+A/680/A28

References

1. Agol, E., Deck, K.M.: Transit timing to first order in eccentricity. ApJ **818**, 177 (2016)
2. Dawson, R.I., Johnson, J.A.: The photoeccentric effect and proto-hot Jupiters I Measuring photometric eccentricities of individual transiting planets. ApJ **756**, 122 (2012)
3. Gorrini, P., et al.: Planetary companions orbiting the M dwarfs GJ 724 and GJ 3988. A CARMENES and IRD collaboration. A&A **680**, A28 (2023)
4. Hadden, S., Lithwick, Y.: Numerical and analytical modeling of transit timing variations. ApJ **828**, 44 (2016)
5. Holst, L.: On the lengths of the pieces of a stick broken at random. J. Appl. Prob. **17**, 623–634 (1980)
6. Linial, I., Gilbaum, S., Sari, R.: Modal decomposition of TTV: inferring planet masses and eccentricities. ApJ **860**, 16 (2018)
7. MacDougall, M.G., Gilbert, G.J., Petigura, E.A.: Accurate and efficient photoeccentric transit modeling. AJ **166**, 61 (2023)
8. Montgomery, D.C., Peck, E.A., Vining, G.G.: Introduction to Linear Regression Analysis, 5th edn. John Wiley & Sons Inc, Hoboken (2012)
9. Mood, A.M., Graybill, F.A., Boes, D.C.: Introduction to the Theory of Statistics, 3rd edn. McGraw-Hill, Tokyo (1974)
10. Myers, R.H., Montgomery, D.C.: Response Surface Methodology: Process and Product Optimization Using Designed Experiments. Wiley, New York (1995)
11. Stevens, W.L.: Solution of a geometric problem in probability. Ann. Eugenics **9**, 315–320 (1939)
12. Tamuz, O., Mazeh, T., North, P.: Automated analysis of eclipsing binary light curves – I. EBAS – a new eclipsing binary automated solver with EBOP. MNRAS 367, 1521–1530 (2006)
13. Tatum, J.: Celestial Mechanics. LibreTexts, Davis (California) (2020)